High-Yield Production of Highly Fluorinated Graphene by Direct Heating Fluorination of Graphene-oxide

Xu Wang,[†] Yunyang Dai,[†] Jie Gao,[†] Jieyang Huang,[†] Baoyin Li,[†] Cong Fan,[†] Jin Yang,[‡] and Xiangyang Liu*,[†]

[†]State Key Laboratory of Polymer Materials Engineering, College of Polymer Science and Engineering, Sichuan University, Chengdu, Sichuan 610065, P.R. China

[‡]State Key Lab of Pulp and Paper Engineering, South China University of Technology, Guangzhou 510640, P. R. China

Ⓢ *Supporting Information*

ABSTRACT: By employing honeycomb GO with large surface area as the starting materials and using elemental fluorine, we developed a novel, straightforward topotactic route toward highly fluorinated graphene in really large quantities at low temperature. The value of F/C molar ratio approaches to 1.02. Few-layer fluorinated graphene sheets are obtained, among which the yield of monolayered FG sheet is about 10% and the number of layers is mainly in the range of 2−5. Variations in morphology and chemical structure of fluorinated graphene were explored, and some physical properties were reported.

KEYWORDS: *fluorinated graphene, chemical structure, direct fluorination*
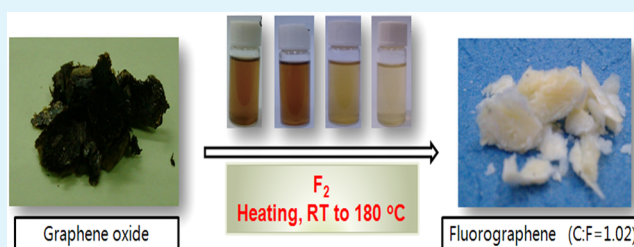
Graphene continues to attract intense interest because of its extraordinary properties, not only the initial studies of graphene's electron transport properties.[1] Chemical modification of graphene, one of the research directions that have emerged recently, is based on the notion of graphene being a giant macromolecule.[2] For example, graphene oxide (GO) is a graphene sheet densely decorated with hydroxyl and other groups, obtained by exposure of graphite to liquid oxidizing agent.[3] However, GO appears to be inhomogeneous with a mixture of regions that are pristine and densely decorated. Graphane is the other one known derivative, which is a theoretically predicted stoichiometric derivative of graphene with a hydrogen atom attached to each carbon atom.[4] This stoichiometric material has been recently synthesized by several groups successfully with both surfaces of graphene exposed to atomic H. Unfortunately, graphane rapidly lost H even at mild temperature, which restricts its usage in applications where stability is required.[5] Fluorinated graphene (FG) has been reported as one more stable graphene derivative by several groups lately.[6,7]

Mechanical cleavage was attempted to extract individual fluorographene sheet from commercially available graphite fluoride, but it was proved surprisingly difficult to get few-layer or monolayered FG sheets.[8−10] Recently, monolayered FG was successfully made by fluorination of graphene with atomic F formed by decomposition of Xenon difluoride.[7] It was reported this fully fluorinated material was an excellent insulator with high thermal and chemical stability. However, the FG sheets were too small for accurate analysis of their chemical composition and structure. Some important structural character have not be reported, such as the nature of C−F bonding, which affects the

performances of carbon fluoride materials to a great degree. This method cannot be used to prepare FG in large scale. Zhaofeng Wang et al. synthesize FG sheets by a simple hydrothermal reaction between GO dispersion and HF, whereas the F content is low.[11]

Some outstanding performances of highly fluorinated graphene (HFG) have been predicted by the theoretical analysis and computer simulation.[12−17] For example, the nanoroads and quantum dots can be patterned on this insulating functionalized graphene.[18,19] Preparation of all-graphene transparent and flexible electronics is feasible by selectively reduction of HFG.[20] However, due to the shortage in synthesis of fluorographene, it is hard to get enough individual FG sheets for device fabrication and experimentally studying for physical and chemical properties, which seriously hinders the development of HFG as advanced materials.

By employing honeycomb GO with large surface area (see Figure S1 in the Supporting Information) as the starting materials and by using the most reactive fluorination agent, elemental fluorine (F_2), we developed a novel, straightforward topotactic route toward HFG in really large quantities at low temperature. The fluorination was carried out in closed stainless steel (SUS316) chamber (10 L) equipped with vacuum line. One hundred milligrams of GO was put in the chamber. After exchanging nitrogen three times, we removed residual oxygen and moisture in the chamber. 90 KPa F_2/N_2 mixed gas was

introduced in to the chamber at room temperature (RT). The F_2 concentration was adjusted to obtain products with different degree of fluorination. The corresponding product was denoted as FGO-1, FGO-2, and FGO-3 for 2%, 5% and 10% F_2 concentration, respectively. Fluorination processed with temperature increasing from RT to a certain temperature (180 °C) at rate of 4 °C/min, and steadied at this temperature for 20 min. More details about experiment are shown in the Supporting Information. The chemical composition and structure of fluorinated samples were characterized by X-ray photoelectron spectroscopy (XPS), Fourier transform infrared spectroscopy (FTIR), Raman, atomic force microscope (AFM), thermogravimetric analysis (TGA), transmission electron microscope (TEM), and ultraviolet visible spectra (UV−vis) etc. The topotactic preparation method presents a general and facile approach to synthesis of fluorinated graphene with a much lower degree of agglomeration than graphite fluoride. It was easy for this material to be exfoliated to obtain few-layer even monolayered FG sheets.

The value of F/C ratio for fluorinated samples increases with F_2 concentration in the process of fluorination, as shown in Table 1. The method of topotactic synthesis gives rise to very high level

Table 1. Chemical Composition of Fluorinated and Nonfluorinated GO Measured by XPS

| sample notation | chemical composition measured by XPS | | | | TGA | chemical formula |
	F (%)	O (%)	C (%)	F/C (±0.01)	ML-peak (°C)	
GO	0	29.88	70.12	0	197.3	$C_1O_{0.426}$
FGO-1	33.41	11.44	55.15	0.65	399.1	$C_1F_{0.65}O_{0.21}$
FGO-2	41.82	8.54	49.64	0.84	418.5	$C_1F_{0.84}O_{0.17}$
FGO-3	48.11	4.5	47.39	1.02	469.7	$C_1F_{1.02}O_{0.09}$

of fluorination. For instance, the values of F/C molar ratio ($R_{F/C}$) observed is as high as 1.02 observed for FGO-3. Even if the F_2 concentration is only 2%, the F/C ratio achieves at 0.65, which is higher than what reported by others previously.[11]

A single layer of FG sheets were deposited on a substrate by simply drop casting from a dilute FGO-3 ($R_{F/C}$ = 1.02) dispersion of alcohol, as shown in Figure 1a. And some TEM pictures are shown in Figure S2 in the Supporting Information. This provides a facile approach to obtain monolayered FG for device fabrication or studies on the properties of individual sheets. Its TEM images (Figure 1b) indicated the monolayer structure. This is further confirmed by the AFM image and thickness of FGS (Figure 1e and 1g), and there are some FG sheets whose thickness is determined to be about 1 nm, suggesting that the FG sheet should be of one layer (Figure 1e). Statistical data have been provided according to AFM image (Figure 1h). The yield of monolayered FG sheet is about 10% and the number of layers is mainly in the range of 2−5, which indicates that the method is an efficient one to provide few layers FG sheets. The selected area electron diffraction pattern in Figure 1d is clearly visible, and the annular structure reveals that the achieved FG sheet is polycrystal. The FG sheet shows irregular atomic arrangement (Figure 1c). This is probably because the smooth and regular surface of graphene sheets is distorted by fluorination, and finally exhibits a chair or boat structure configuration (sp3-hybridized carbon).[11] This is confirmed by infrared spectroscopy (Figure 3) and results showed the presence of a very intense band at 1221 cm^{-1} characteristic of a C−F covalent bond. Another reason may be that the composition of fluorinated graphene in this study is close but not stoichiometric, even through the value of F/C molar ratio is about 1.

The FG sheets shows hydrophobicity due to high fluorine content (as shown Figure 1S in the Supporting Information), so they are not able to be dispersed in water. Therefore, the fluorinated and nonfluorinated samples were dissolved in alcohol, getting dispersed. The large size of the conjugated π
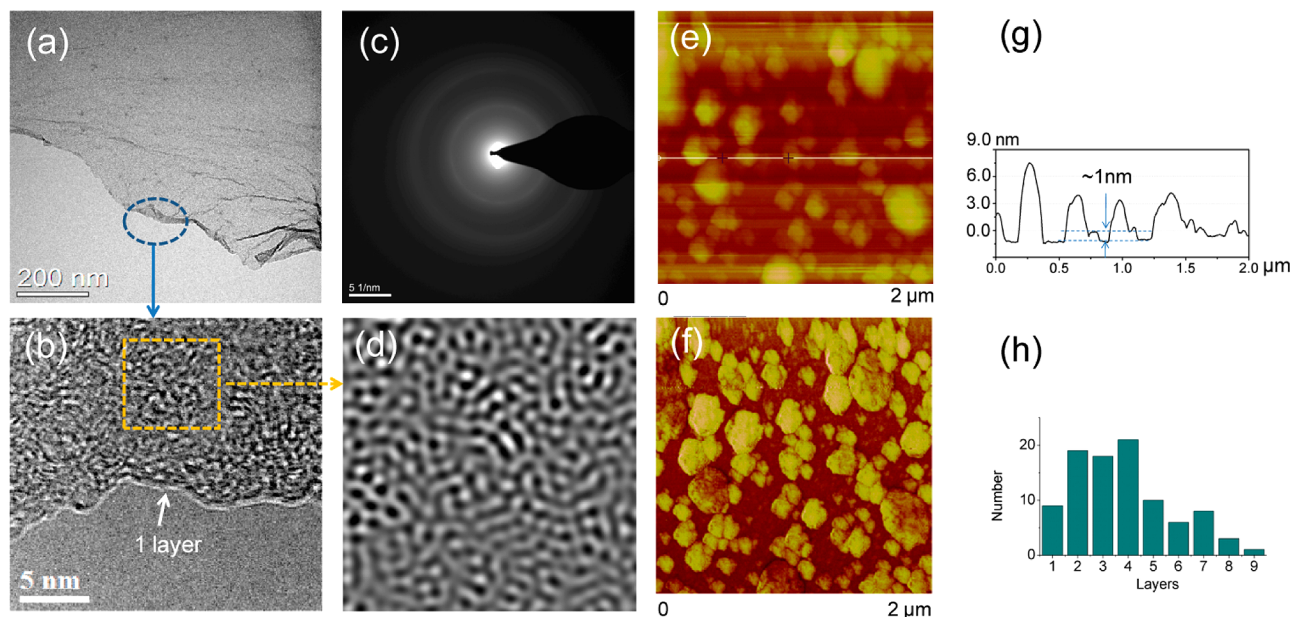

Figure 1. (a) TEM and (b) HRTEM micrographs of the highly fluorinated sample FGO-3. (c) Selected area electron diffraction pattern. (d) Magnified image of the yellow section in panel b. (e, f, g) The AFM image, corresponding phase diagram, and thickness of FGS. (h) Statistic data of layers of FG sheets.
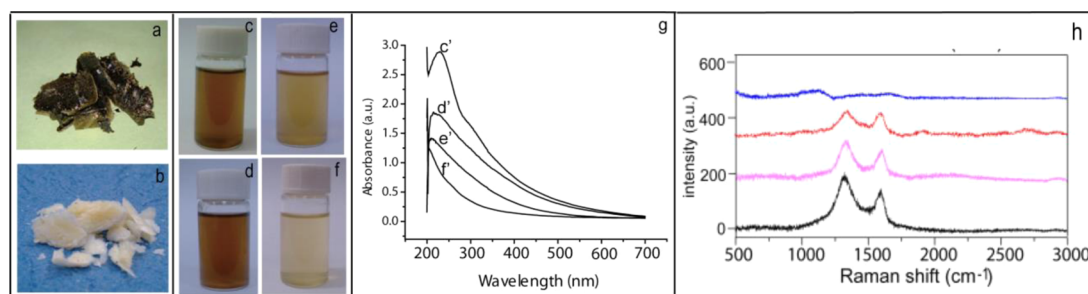
Figure 2. Photographs and UV−vis spectra of the solutions of fluorinated and nonfluorinated GO. (a) A photograph of GO. (b) Photograph of FGO-3. (c) Photograph of the aqueous solution (1 mg/mL) of GO. (d−f) Photographs of the alcoholic solution (1 mg/mL) of FGO-1, FGO-2, and FGO-3, respectively. (g) UV−vis spectra of the solution of GO (c′), FGO-1 (d′), FGO-2 (e′), and FGO-3 (f′). (h) Raman spectra of fluorinated and nonfluorinated samples: FGO-3, FGO-2, FGO-1, and GO (top to bottom).
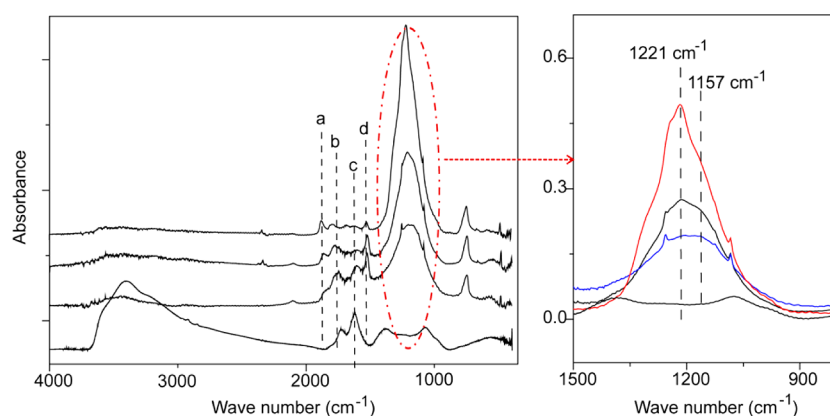

Figure 3. FTIR spectra of fluorinated and nonfluorinated samples: FGO-3, FGO-2, FGO-1, and GO (top to bottom).
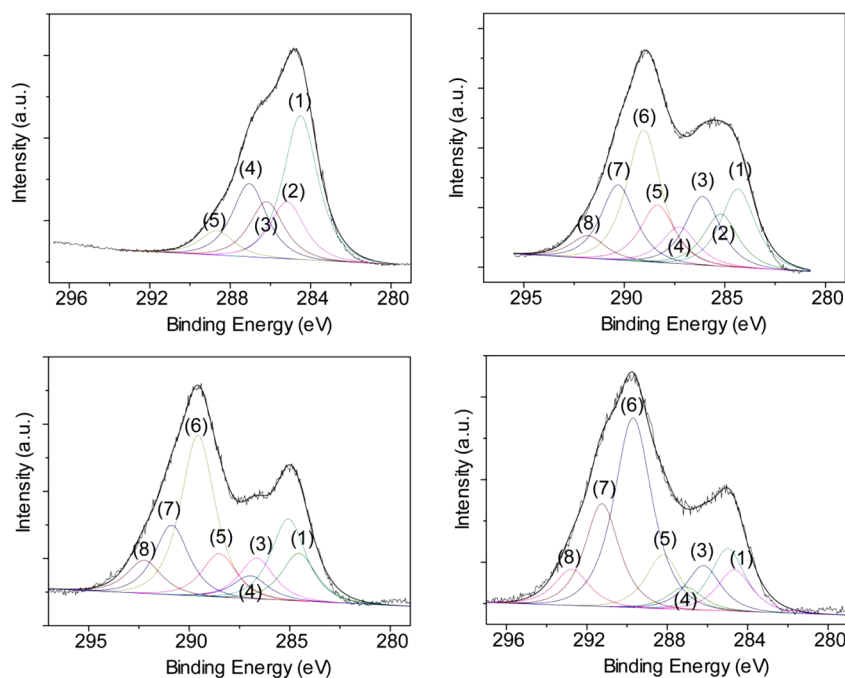

Figure 4. Curve-fitting of XPS C 1s spectrum of FGO-3.

domains and some chromophores determined that the GO was brown.[21] Although the GO and FGO-1 solution is dark brown, the FGO-2 is yellow, and the FGO-3 is almost colorless.

Figure 2g shows the UV−vis spectra of the solutions of fluorinated and nonfluorinated GO. The SGO spectrum has the

characteristic maximum at 200−300 nm region, which is consistent with the literature data.[21,22] The absorbance in this region is often attributed to conjugated ketones. The absorbance in the 270−350 nm region is thought to be caused by the conjugated aromatic domains. In contrast, the absorption peaks

Table 2. Location, Ascription, and Content of Chemical Groups in Fluorinated and Nonfluorinated Samples

	peak	(1)	(2)	(3)	(4)	(5)	(6)	(7)	(8)
GO	location (eV)	284.5	285.2	286.2	287.1	288.7			
	ascription	−C=C−	−$\underline{C}$−	$\underline{C}$−O	C=O	$\underline{C}$OO			
	content (%)	40.6	16.1	15.8	20.6	6.9			
FGO-1	location (eV)	284.4	285.2	286.1	287.3	288.3	289.0	290.3	291.8
	ascription	−C=C−	−$\underline{C}$−	$\underline{C}$-O	C=O	C_{sp2}-F	C−F	CF_2	CF_3
	content (%)	15.0	10.0	13.2	7.0	10.9	25.2	14.4	4.3
FGO-2	location (eV)	284.6	285.1	286.2	287.0	288.6	289.7	291.1	292.4
	ascription	−C=C−	−$\underline{C}$−	$\underline{C}$−O	C=O	C_{sp2}-F	C−F	CF_2	CF_3
	content (%)	12.2	11.5	8.0	7.1	10.0	32.6	13.4	5.2
FGO-3	location (eV)	284.6	285.0	286.2	287.1	288.2	289.7	291.2	292.7
	ascription	−C=C−	−$\underline{C}$−	$\underline{C}$−O	C=O	C_{sp2}−F	C_{sp3}−F	CF_2	CF_3
	content (%)	7.2	10.8	7.8	4.0	9.4	37.6	16.9	6.3

of the fluorinated sample at the two regions and their absorption in the whole spectral region (>350 nm) decrease with fluorine concentration in the process of fluorination. The colorless FGO-3 solution almost does not absorb in the 400−800 nm, and its absorbance in the 270−350 nm region is very weak. This indicates that the electronic conjugation within the GO sheets is destroyed by fluorination. In additional, the Raman spectra of samples with different degree of fluorination are shown in Figure 2h. One can be seen that partially fluorinated samples (FGO-1 and FGO-2) exhibits the Raman spectra that resemble that of GO. They has comparable intensities of the G and D peaks and very small D* band. However, all the Raman features gradually disappear in the spectrum of FGO-3. The disappearance of all the characteristic peaks clearly proves dramatic changes induced by fluorination. That is, almost all of sp^2-hybridized carbon in the aromatic regions converts sp^3 carbon for FGO-3. This result is in agreement with previous report, which is explained by complete optical transparency of FGO-3 fluorinated graphene sheets to the laser light.[7] Thus, it is useful to control fluorine content to tailor its electronic conjugation level, which could be further used to get different optical and electrical properties of the fluorinated carbon materials.

Chemical structure of fluorinated and nonfluorinated samples was measured by FTIR and XPS. Some important structural character, such as nature of C−F bonding, have not be reported due to the low yield of FG. As shown in Figure 3, the evolution of the vibration frequencies ν(C−F) is a function of the F content of the final fluorinated products. For FGO-1, the C−F bonding is of two natures. When the fluorine atom is linked with sp^3-hybridization, the C−F bond is considered as covalent bonding, with the stretching vibration absorption corresponding to the peak at 1221 cm^{-1}. Its intensity increases obviously with increasing $R_{F/C}$, and forms a strong peak at 1221 cm^{-1} in spectrum of FGO-3. The broad band centered at about 1150 cm^{-1} indicates the presence of another kind of C−F bond, which is generally called as semi-ionic C−F bonds as in graphite and carbon nanotube fluoride synthesized at low temperature.[23,24] It is considered that the carbon atoms retain a degree of sp^2-hybridization for this C−F bond (hereafter referred to as "C_{sp2}−F"). Corresponding C1s peaks of XPS spectra were also investigated in Figure 4, and assignments are listed in Table 2. The C 1s curve fit spectrum of fluorinated samples exhibits two components corresponding to groups C−F bonds, peak (5) at about 288 eV and peak (6) at 289 eV, which are assigned to covalent C−F bond and C_{sp2}−F, respectively. The intensity of peak (5) component increases obviously with fluorination degree, while that of C_{sp2}−F shows a slight decrease. This

decrease maybe arises from the reducing of the conjugated π domains. Meanwhile the share of CF_2 and CF_3 components has some increases, but not very large. Thus, the raising of fluorination degree is in the form of an increasing of C−F covalent bond.

The peaks of absorption around 3000−3650 cm^{-1}, corresponding to the stretching vibration of H−R, almost have disappeared after fluorination, even for a low F_2 concentration (2%). It is inferred that these hydrogen bonds (H−R) are substituted by fluorine bonds (F−R). The hydrogen atoms bonding on the organic macromolecules (C−H and O−H) are easily substituted by fluorine atoms,[25,26] and product HF which is able to catalyze the fluorination of carbon materials.[27] Catalysis of HF could probably contribute to the appearance of C_{sp2}-F bonds, for the previous reports which have shown that the catalyzed fluorination at low temperature would produce semi-ionic C−F bonds.[28−30]

The 1530 cm^{-1} bands (Figure 3d) corresponds to stretching vibrations of in-plane C=C bonds in aromatic region which are progressively broken. These bands almost disappear in the spectrum of FGO-3, indicating the aromatic regions were gradually fluorinated. This can be seen as the rate-limiting step of the whole fluorination process. This is further confirmed by the XPS data, and the −C=C−content (peak 1 in Figure 4, Table 2) has been decreased with rising of fluorination level.

The contents of oxygen in fluorinated samples decrease evidently becaues of the occurrence of thermal reduction and introduction of fluorine into fluorinated samples, while the intensity of peaks at about 1740 and 1620 cm^{-1} (Figure 3b, c) assigned to −C=O and C−O groups weakens obviously in infrared spectra with increasing of fluorine content. Actually, the oxygen content is mainly influenced by three factors: thermal reduction of GO resulting in elimination of oxygen related groups; substitution of oxygen related groups by fluorine atom;[31] residual oxygen gas in fluorine gas taking part in fluorination, producing new groups containing oxygen such as −C(O)F group. The band at 1840 cm^{-1} (Figure 3a) is due to the ν(C=O) stretching of −C(O)F groups.[32] The hydrolysis of the −C(O)F group is very favorable, and intrinsic traces of water in air result in the formation of the −COOH group. Due to hydrophobicity of the HFG, the 1840 cm^{-1} band characteristic of the −C(O)F group is observed.

The increasing of F content results in the position of F peak shifting from 687.9 to 688.9 eV (Figure S3 in Supporting Information), implying the enhancing of C−F covalence, which is consistent with the results of FTIR analysis. The higher C−F covalence is good for the chemical stability of fluorinated carbon

8297

dx.doi.org/10.1021/am402958p | *ACS Appl. Mater. Interfaces* 2013, 5, 8294−8299

Table 3. Chemical Composition of Fluorinated Graphene Prepared under Different Conditions

sample number	fluorinating conditions				chemical composition measured by XPS		
	fluorine concentration (%)	heating rate (°C/min)	maximum temperature (°C)	holding times (min)	F content (%)	O content (%)	C content (%)
1	5	0	RT	120	15.50	21.41	63.09
2	5	4	100	40	30.60	17.52	51.88
3	5	4	180	60	41.82	8.54	49.64
4	5	4	250	0	48.11	4.5	47.39
5	5	4	180	0	38.80	10.40	50.80
6	5	4	180	20	41.82	8.54	49.64
7	5	4	180	60	42.10	8.19	49.71

materials.[33,34] In order to validate the effect of nature of C−F bonding on stability of materials, thermal stability of GO and fluorinated samples described above has been followed by thermogravimetric analysis up to 800 °C (Figure S3 and Table S1 in the Supporting Information). The rapid weight loss observed around 197 °C is attributed to the elimination of oxide related group bonding on the graphene sheets. After fluorination, the thermal stability of samples was improved significantly. Taking FGO-3 for example, the weight loss mainly occurred at 470 °C.

As a gas−solid reaction, diffusion of F_2 seriously influences fluorination degree of the final products. The diffusion is generally determined by reaction temperature and time which has strong effect on chemical composition and structure of the final fluorinated samples. As shown in Table 3, variation of fluorinating temperature results in major changes of F content. At a low temperature (RT), the F content is not larger than 16%, even after a long reaction time. With increasing temperature, the value increases significantly. When maximum temperature of fluorination is raised to 250 °C, the value of the F/C ratio could achieve 1 even with only 5% F_2 concentration.

It is worth noting that the O content reduces obviously at RT after fluorination, and the reduction amount is about the same than the F content. Meanwhile, the share of −C≡C− component has no obvious change according to curve-fitting of the XPS C 1s spectrum of sample 1 (see Figure S5 and Table S2 in Supporting Information). Combining with our recent work on fluorination of CNTs,[31] it seems that the oxygen related groups bonding to the carbon materials could provide reactive sites for the fluorination in the fluorine gas atmosphere.

However, the variation of holding times at maximum temperature lead to only slight changes in the fluorinated degree, when F_2 concentration and maximum temperature are constant. That is mainly because of the honeycomb structure of GO resulted from freeze-drying. The large surface area and interlayer space of GO makes it possible for molecular F_2 having a good contact with GO sheets, which blunts the impact of reaction times.

On the basis of effects of fluorine concentration, fluorination time and temperature on chemical structure of fluorinated samples, it seems that reaction temperature plays a more important role in determination of the fluorination degree. In the process of direct heating-fluorination, the amorphous region containing the oxygen related groups easily reacts with fluorine gas even at low temperature, while the aromatic region is progressively fluorinated at a higher temperature. Furthermore, oxygen content decreased further with increasing temperature. That is to say, the final chemical structure of FG is mainly controlled by thermodynamic factor and impacted by dynamic factors simultaneously. However, the intricate reactive mechanism of the fluorination is still unclear, so the central focus of our future research is to investigate the mechanism and preparation of the stoichiometric FG with a large size.

■ ASSOCIATED CONTENT

Ⓢ Supporting Information

Experimental section, SEM pictures of honeycomb GO; photograph of a 15-μm-thick FGO-3 film; F 1s spectra of fluorinated samples; data of thermal analysis; TGA and DTA lines; data of thermal analysis; curve-fitting of XPS C 1s spectrum of sample 1 in Table 3 in manuscript; location, ascription, and content of sample 1. This material is available free of charge via the Internet at http://pubs.acs.org.

■ AUTHOR INFORMATION

Corresponding Author
*E-mail: lxy6912@sina.com.

Notes
The authors declare no competing financial interest.

■ ACKNOWLEDGMENTS

■ REFERENCES

(1) Geim, A. K.; Novoselov, K. S. *Nat. Mater.* **2007**, 6, 183−191.

(2) Ruoff, R. *Nat. Nanotechnol.* **2008**, 3, 10−11.

(3) Park, S.; Ruoff, R. S. *Nat. Nanotechnol.* **2009**, 4, 217−224.

(4) Sofo, J. O.; Chaudhari, A. S.; Barber, G. D. *Phy. Rev. B* **2007**, 75, 153401−153404.

(5) Elias, D. C.; Nair, R. R.; Mohiuddin, T. M. G.; Morozov, S. V.; Blake, P.; Halsall, M. P.; Ferrari, A. C.; Boukhvalov, D. W.; Katsnelson, M. I.; Geim, A. K.; Novoselov, K. S. *Science* **2009**, 323, 610−613.

(6) Zbořil, R.; Karlický, F.; Bourlinos, A. B.; Steriotis, T. A.; Stubos, A. K.; Georgakilas, V.; Šafářová, K.; Jančík, D.; Trapalis, C.; Otyepka, M. *Small* **2010**, 6, 2885−2891.

(7) Nair, R. R.; Ren, W.; Jalil, R.; Riaz, I.; Kravets, V. G.; Britnell, L.; Blake, P.; Schedin, F.; Mayorov, A. S.; Yuan, S.; Katsnelson, M. I.; Cheng, H. M.; Strupinski, W.; Bulusheva, L. G.; Okotrub, A. V.; Grigorieva, I. V.; Grigorenko, A. N.; Novoselov, K. S.; Geim, A. K. *Small* **2010**, 6, 2877−2884.

(8) Novoselov, K. S.; Jiang, D.; Schedin, F.; Booth, T. J.; Khotkevich, V. V.; Morozov, S. V.; Geim, A. K. *Proc. Natl. Acad. Sci. U.S.A.* **2005**, 102, 10451−10453.

(9) Cheng, S. H.; Zou, K.; Okino, F.; Gutierrez, H. R.; Gupta, A.; Shen, N.; Eklund, P. C.; Sofo, J. O. *Phys. rev. B* **2010**, 81, 205435−205439.

(10) Worsley, K. A.; Ramesh, P.; Mandal, S. K.; Niyogi, S.; Itkis, M. E.; Haddon, R. C. *Chem. Phys. Lett.* **2007**, 445, 51−56.

(11) Wang, Z. F.; Wang, J. Q.; Li, Z. P.; Gong, P. W.; Liu, X. H.; Zhang, L. B.; Ren, J. F.; Wang, H. G.; Yang, S. G. *Carbon* **2012**, *50*, 5403−5410.
(12) Withers, F.; Russo, S.; Dubois, M.; Craciun, M. *Nanoscale Res. Lett.* **2011**, *6*, 526−536.
(13) Robinson, J. T.; Burgess, J. S.; Junkermeier, C. E.; Badescu, S. C.; Reinecke, T. L.; Perkins, F. K.; Zalalutdniov, M. K.; Baldwin, J. W.; Culbertson, J. C.; Sheehan, P. E.; Snow, E. S. *Nano Lett.* **2010**, *10*, 3001−3005.
(14) Withers, F.; Bointon, T. H.; Dubois, M.; Russo, S.; Craciun, M. F. *Nano Lett.* **2011**, *11*, 3912−3916.
(15) Kwon, S.; Ko, J. H.; Jeon, K. J.; Kim, Y. H.; Park, J. Y. *Nano Lett.* **2012**, *12*, 4043−4048.
(16) Li, Y.; Li, F.; Chen, Z. *J. Am. Chem. Soc.* **2012**, *134*, 11269−11275.
(17) Ribas, M.; Singh, A.; Sorokin, P.; Yakobson, B. *Nano Res.* **2011**, *4*, 143−152.
(18) Şahin, H.; Topsakal, M.; Ciraci, S. *Phys. Rev. B* **2011**, *83*, 115432−115437.
(19) Shen, N.; Sofo, J. O. *Phys. Rev. B* **2011**, *83*, 245424−245429.
(20) Ueta, A.; Tanimura, Y.; Prezhdo, O. V. *J. Phys. Chem. C* **2012**, *116*, 8343−8347.
(21) Dimiev, A.; Kosynkin, D. V.; Alemany, L. B.; Chaguine, P.; Tour, J. M. *J. Am. Chem. Soc.* **2012**, *134*, 2815−2822.
(22) Li, D.; Muller, M. B.; Gilje, S.; Kaner, R. B.; Wallace, G. G. *Nat. Nanotechnol.* **2008**, *3*, 101−105.
(23) Hamwi, A.; Daoud, M.; Cousseins, J. C. *Synth. Met.* **1988**, *26*, 89−98.
(24) Hamwi, A.; Alvergnat, H.; Bonnamy, S.; Guin, F. B. *Carbon* **1997**, *35*, 723−728.
(25) Kharitonov, A. P. *J Fluorine Chem.* **2000**, *103*, 123−127.
(26) Kharitonov, A. P. *Prog. Org. Coatings* **2008**, *61*, 192−204.
(27) Zhang, W.; Bonnet, P.; Dubois, M.; Ewels, C. P.; Guérin, K.; Petit, E.; Mevellec, J. Y.; Vidal, L.; Ivanov, D. A.; Hamwi, A. *Chem. Mater.* **2012**, *24*, 1744−1751.
(28) Sato, Y.; Itoh, K.; Hagiwara, R.; Fukunaga, T.; Ito, Y. *Carbon* **2004**, *42*, 3243−3249.
(29) Banerjee, S.; Hemraj, B. T.; Wong, S. S. *Adv. Mater.* **2005**, *17*, 17−29.
(30) Guérin, K.; Pinheiro, J. P.; Dubois, M.; Fawal, Z.; Masin, F.; Yazami, R.; Hamwi, A. *Chem. Mater.* **2004**, *16*, 1786−1792.
(31) Wang, X.; Chen, Y.; Dai, Y. Y.; Wang, Q.; Gao, J.; Huang, J. Y.; Yang, J.; Liu, X. Y. *J. Phys. Chem. C* **2013**, *117*, 12078−12085.
(32) Solomun, T.; Schimanski, A.; Sturm, H.; Illenberger, E. *Macromolecules* **2005**, *38*, 4231−4236.
(33) Touhara, H.; Okino, F. *Carbon* **2000**, *38*, 241−267.
(34) Parmentier, J.; Schlienger, S.; Dubois, M.; Disa, E.; Masin, F.; Centeno, T. A. *Carbon* **2012**, *50*, 5135−5147.